Prolonged Dynamic Support from the Icelandic Plume of the North East Atlantic Margin

Jonathon P.A. Hardman[1], Nick Schofield[1], David W. Jolley[1], Simon P. Holford[2], Adrian J. Hartley[1], Stephen Morse[3], John Underhill[4], Douglas A. Watson[1], Eva H. Zimmer[1]

[1]*Department of Geology and Petroleum Geology, University of Aberdeen, Aberdeen, AB24 3FX, UK*

[2]*Australian School of Petroleum, University of Adelaide, Adelaide, SA 5005, Australia*

[3] *Lyme Bay Consulting, Yew tree House, Lewes Road, Forest Row, East Sussex, RH18 5AA, formerly at PGS, Weybridge, Surrey, KT13 0NY, UK*

[4]*Shell Centre for Exploration Geoscience, Heriot-Watt University, Edinburgh, EH14 4AS, UK*

Abstract: Sedimentary basins affected by hotspots often contain records of uplift and subsidence within coeval stratigraphic successions. The subsidence history can contain measureable perturbations in ancient palaeogeographies that can help constrain the duration of dynamic support. ~56 Ma the North East Atlantic experienced uplift related to the Iceland mantle plume. Within the Faroe-Shetland Basin, we document the stratigraphic record of subsidence following plume uplift, through integration of regional seismic datasets and well data. Subsidence following plume uplift is recorded by mapping the southward migration of palaeocoastlines throughout the early Eocene of the Faroe-Shetland Basin. We find that after initial uplift over 0.5 Ma, subsidence was inhibited for 0.45 Ma. Coeval with initiation of rifting in the North Atlantic, at 54.9 Ma, a ~0.9 Ma period of accelerated subsidence occurred, recorded by migration of the coastline by ~80 km inland. We attribute these events to a prolonged period (2 Ma) of dynamic support from the Iceland plume terminated by rapid loss of dynamic support coeval with rifting in the Northeast Atlantic, 54.9 Ma. Our results suggest that palaeogeographical analysis is a powerful tool in constraining the duration of dynamic support in basins affected by mantle plumes.

Dynamic uplift and subsidence resulting from mantle convection affects rift-basins globally (White & Mckenzie, 1989; Calves *et al.*, 2008; Braun, 2010). Dynamic topography can exert a

strong control on the sedimentary and stratigraphic record through the development of uplift-related unconformities and dynamic compensation of the post-uplift sedimentary record (Clift & Turner, 1998; Tindale, 1998; Lin *et al.*, 2003; Reeve *et al.*, 2016). The timing of uplift can be difficult to unravel, as it is recorded in the subaerial erosion of uplifted rocks, where uplift is sufficient (Lin *et al.*, 2003; Shaw Champion *et al.*, 2008). The subsidence history, however, contains paleolandscapes from which measureable perturbations in ancient paleogeographies can be used to constraint the duration (transient or long-lived) and mechanisms of dynamic support (Braun, 2010).

At ~63 Ma, uplift of the north east Atlantic commenced (White & Mckenzie, 1989; Brodie & White, 1994; Nadin & Kusznir, 1995). The effects of this uplift are observed throughout large parts of Northwest Europe, from Greenland to the North Sea (Bertram & Milton, 1989; Jones & Milton, 1994; Nadin & Kusznir, 1995; Clift & Turner, 1998; Dam *et al.*, 1998; Stucky de Quay *et al.*, 2017). In the Faroe-Shetland Basin, located offshore Northwest Scotland (Fig. 1), a ~56.1 Ma unconformity with a total relief of 550 m has been mapped over an 8000 km^2 area throughout the southern Faroe-Shetland Basin (Smallwood & Gill, 2002; Shaw Champion *et al.*, 2008; Hartley *et al.*, 2011). The timing of this event, concomitant with extensive volcanism, has led authors to link uplift throughout the north east Atlantic to the impingement of the Iceland mantle plume on the North Atlantic region (Bertram & Milton, 1989; Turner & Scrutton, 1993; Brodie & White, 1994; Hall & White, 1994; Nadin & Kusznir, 1995; White, 1997; White & Lovell, 1997). However, inconsistencies exist in the record of subsidence between ~56 to 54 Ma in the Faroe-Shetland Basin. Hartley et al. (2011) proposed that following 1 million years of subaerial exposure, the Faroe-Shetland Basin was reburied rapidly. Contrasting this, prolonged dynamic support following uplift has been recognised in the Faroe-Shetland Basin through thermochronology (Nadin *et al.*, 1997), basin modelling (Fletcher *et al.*,, 2013), backstripping (Clift & Turner, 1998) and analysis of 3D seismic data

(Smallwood & Gill, 2002; Shaw Champion *et al.,* 2008), with reestablishment of marine conditions in the Faroe-Shetland Basin notably occurring after deposition of the Balder Formation, ~1.5–2.0 Ma following uplift (Rudge *et al.*, 2008). However, no attempt has been made to constrain the timing and rate of subsidence through analysis of the post-uplift palaeogeographies and, hence, constrain the duration and nature of dynamic support in the Faroe-Shetland Basin.

Here, we detail the post-volcanic succession of the Faroe-Shetland Basin, where the non-marine to shallow marine Ypresian-aged Flett, Balder and Horda Formations record the landward migration of the coastline towards the UK mainland. We map the successive positions of the coastline in the southern Faroe-Shetland Basin. Through depth conversion, decompaction and relative age dating of the sequences using biostratigraphy, we assign ages and depths to the palaeocoastlines to estimate the rate of subsidence throughout the Late Palaeocene and Early Eocene. We find that the rate of subsidence provides detailed constraints on the duration and effect of dynamic support resulting from impingement of the Iceland mantle plume on the Northeast Atlantic. Subsidence in the Faroe-Shetland Basin did not occur immediately over a period of ~1 Ma, as was previously constrained (Hartley *et al.*, 2011), rather, subsidence was initially protracted and inhibited, before occurring rapidly over a 0.9 Ma period of time coeval with the initiation of rifting in the North Atlantic at 54.9 Ma (Pitman & Talwani, 1972). This rapid subsidence is inferred to be evidence for a loss of dynamic support in the Faroe-Shetland Basin.

REGIONAL GEOLOGY

Located on the north-east Atlantic margin, the Faroe-Shetland Basin is a 400x200 km wide, NE-SW trending complex of sub-basins and intra-basinal highs (Duindam & Hoorn, 1987) (Fig. 1). Following the close of the Caledonian orogeny, the North East Atlantic was influenced by

79 periods of episodic rifting throughout the late Palaeozoic to Mesozoic (Dore *et al.*, 1999). The
80 Faroe-Shetland Basin formed during a 70 Ma period of episodic rifting in the Cretaceous from
81 the Valanginian through to the Maastrichtian (Dean *et al.*, 1999; Lamers & Carmichael, 1999).
82 Cretaceous rifting was superseded by Late Cretaceous to early Palaeocene post-rift
83 subsidence (Turner & Scrutton, 1993), during which marine conditions prevailed throughout
84 the Faroe-Shetland Basin (Lamers & Carmichael, 1999).

85 The earliest evidence for activity related to the Iceland hotspot is recorded by the
86 63.24 Ma Lower Basalt Formation on Antrim, Northern Ireland (Ganerød *et al.*, 2010).
87 Volcanism latterly centred on the British Tertiary Volcanic Province as volcanism migrated
88 north, 63-62 Ma (Pearson *et al.*, 1996; Chambers & Pringle, 2001; Storey *et al.*, 2007). At ~59.2
89 Ma, a major increase in volcanic activity is recorded by regional deposition of the Kettla Tuff
90 Member (Jolley & Bell, 2002; Watson *et al.*, 2017) and the eruption of isolated volcanic centres
91 in the north of the Faroe-Shetland Basin (Jolley, 2009; Schofield *et al.*, 2017). Emplacement of
92 an extensive suite of basaltic intrusions, the Faroe-Shetland Sill Complex, took place, in parts,
93 during this phase of activity (Smallwood & Maresh, 2002; Schofield *et al.*, 2017).

94 A second, main extrusive phase of volcanism began at ~56 Ma with the emplacement
95 of the Faroe Islands Basalt Group (Passey & Jolley, 2008). Prior to, and synchronous with, the
96 eruption of the first lavas, the Faroe-Shetland Basin experienced dynamic uplift with an aerially
97 extensive unconformity surface developing in the Judd and Foinaven Sub-Basins (Shaw
98 Champion *et al.*, 2008). Ypresian–aged, Flett to Balder Formation fluvial systems incised into
99 Thanetian deltaic sedimentary rocks of the Lamba Formation, have provided transient uplift
100 estimates of ~1 km through the modelling of reconstructed drainage patterns (Hartley *et al.*,
101 2011). At ~54.9 Ma, eruption of the Faroe-Islands Basalt Group ceased (Passey & Jolley, 2008)
102 and volcanic activity focused on the incipient Northeast Atlantic rift between the Faroe Islands
103 and Greenland to the north. Flooding of the nascent rift led to phreatomagmatic eruptions

and widespread deposition of the airfall tuffs of the Balder Formation at ~54.5 Ma (Watson *et al.*, 2017).

DATA AND METHODS

Seismic data

An extensive catalogue of 3D seismic data has been used to map the Upper Palaeocene to Lower Eocene post-volcanic succession of the Faroe-Shetland Basin (Fig. 1). This study uses two time-migrated 3D seismic reflection surveys that cover an area of >25 000 km^2; the Faroe-Shetland Basin 2011/2012 Geostreamer© survey (Tenghamm *et al.*, 2008) and the Faroe-Shetland Basin Megasurvey.

The main dataset used in this study is the PGS/TGS FSB2011/12 MultiClient GeoStreamer® survey. Typically, conventional streamers suffer from near surface noise created by ocean waves. These create ghosts, short-path multiples that interfere at particular frequencies, dependent on streamer depth, attenuating parts of the frequency range. The Geostreamer® is a dual sensor marine streamer comprising of co-located hydrophones and vertical particle motion sensors that record both the upcoming and downgoing wavefield information, allowing for removal of the ghosts (Tenghamn *et al.*, 2008). Typically, the Geostreamer® is towed at depths of 15–25 m. The FSB2011/2012 Geostreamer® survey was shot with 12, 6000 m long streamers separated by 75 m (PGS, 2017). The shot interval during acquisition was 75 m.

Several processing techniques were used on the Geostreamer® data, prior to stacking of the seismic data. A dual sensor wave field separation, 3D surface-relation multiple elimination and a high-resolution Radon demultiple were used to reduce the impact of multiples and noise on the seismic data (Day *et al.*, 2013; Dedem & Verschuur, 1998 and Hargreaves *et al.*, 2001, respectively). To stack the data, an anisotropic Kirchhoff pre-stack

129 time migration was used (Kirstiansen *et al.*, 2003). Following processing of the data, the bin
130 dimensions are 12.5 x 18.75 m (PGS, 2017). The interpretation conducted within this study
131 was undertaken using the Final Kirchhoff PSTM Stack that has been waveshaped to zero phase.
132 The data used within this study is of the time domain only and displayed with a reverse
133 polarity, whereby a downward increase in acoustic impedance corresponds to a negative
134 amplitude (red) reflection and a downward decrease in acoustic impedance is represented by
135 a positive amplitude (blue) reflection. The sandstone rich successions in the area typically have
136 an interval velocity of ~2800 ms^{-1} (taken 2400 m measured depth in exploration well 6004/12-
137 1) with a dominant frequency of ~30 Hz. These values were used to calculate a vertical
138 resolution of ~23 m in the vicinity of the Westray High (Fig. 1).
139
140 *Stratigraphy*
141 To constrain the timing and rate of subsidence following uplift, 34 hydrocarbon exploration
142 and discovery wells were used for lithological, petrophysical and palynological analysis. To
143 provide consistency with previous studies in the region, existing stratigraphical schemes have
144 been adopted. The most widely used Palaeocene stratigraphical scheme West of Shetlands is
145 BP's T-Sequence scheme (Ebdon et al., 1995). The T-Sequence scheme was developed
146 through regional sequence mapping in conjunction with biostratigraphy, heavy mineral
147 analysis, sedimentology and lithofacies (Ebdon *et al.*, 1995). Following analysis, the Lower
148 Tertiary of the Faroe-Shetland Basin was divided into a series of sequences, of which T38–
149 T60 are discussed within this manuscript.
150 T-sequences are used in conjunction with Knox et al.'s (1997) lithostratigraphic
151 nomenclature to refer to key formations (Fig. 3). Lithologically, the Sequence T45-T60
152 succession can be difficult to separate into individual formations. Therefore, particular
153 emphasis is placed on biostratigraphical data, which is key in separating the Sequence T40 to

Sequence T60 boundaries. Typically, the sequence consists of a heterogeneous sequence of sands, silts and muds with shallowing upwards trends typical of fluvial, deltaic and coastal plain sequences (Fig. 3). Coals are also observed inland of the mapped palaeocoastlines.

In order to highlight the changes in sedimentary environments throughout the post-volcanic succession, five horizons ranging in age from Sequence T45 to T60 have been mapped (Fig. 4). The 5 horizons mapped are the most regionally extensive throughout the area. To highlight geomorphological features more clearly, horizons are displayed using a blend of RMS amplitude (taken over a window of 10 ms) and variance, explained in detail in Figure 4. The Faroe-Shetland Basin 2011/2012 Geostreamer© survey (e.g. Tenghamm *et al.*, 2008) was used to produce spectral decompositions of the palaeocoastline (Fig. 5). Spectral decomposition generates a number of frequency bands from the original seismic data. RGB spectral decomposition involves assigning three frequency magnitude volumes to three colour channels; red, green and blue. RGB Spectral decomposition for the frequency bands of 13 Hz, 20 Hz and 29 Hz was undertaken using GeoTeric's spectral decomposition software. RGB spectral decomposition is particularly useful for identifying geomorphological features such as channels (Partyka *et al.*, 1999). In this case, fluvial features in the south west of the survey and strand plains positioned adjacent to the palaeocoastline are particularly well imaged (Fig. 5).

DELINEATION OF THE UPPER PALAEOCENE TO LOWER EOCENE SUCCESSION WITHIN THE FAROE-SHETLAND BASIN

Lamba Formation (Thanetian 58.5–56 Ma)

The Lamba Formation records the first major progradation of the palaeoshoreline. It consists of deltaic to marine deposits and 500 m high clinoforms marking the location of the shelf edge at the end of the Thanetian, 56 Ma (Smallwood & Gill, 2002). The base of the Lamba is marked by the Kettla Tuff, a semi-regionally deposited volcaniclastic unit (Watson *et al.,* 2017). The

association between volcanism and progradation of the shelf edge has led previous authors to attribute the Lamba Formation to uplift related to the Iceland Plume (Shaw Champion *et al.*, 2008).

Lower Flett Formation (Ypresian 56.1–55.2 Ma)

Deposition of the lowest Flett Formation, Sequence T40 began following uplift of the Faroe-Shetland Basin and incision of the major Sequence T38/T40 unconformity in the Foinaven and Judd Sub-Basins into underlying formations, at ~56.1 Ma (Smallwood & Gill, 2002; Champion, 2008). Owing to this uplift, the base of the Sequence T40 Flett Formation is marked by a Type one sequence unconformity; a relative fall in sea level below the position of the Sequence T38 shoreline (Van Wagoner, 1988; Ebdon et al., 1995). Deposition of T40 sediments was synchronous with emplacement of the Faroe-Islands Basalt Group with development of siliciclastic sequences taking place during periods of quiescent volcanic activity (Duncan *et al.*, 2009; Schofield & Jolley, 2013). Deposition of the Sequence T40 Flett Formation outside of the volcanic succession occurred only in the topographically lowest reaches of the incised drainage system (Shaw Champion et al. 2008) and is typically marked by fluvial successions, such as conglomerates in exploration well 204/18- 1.

Lower Sequence T40 (unit F1a) is marked in the Corona basin by *Alisocysta margarita* (exploration well 6005/15- 1) (Jolley, 2009). These specimens favour outer neritic and basinal settings (Jolley, 1998) and are typically preserved in mudstone sequences such as those in West Greenland (Nøhr-Hansen et al., 2002). In the Faroe-Shetland Basin, reworking of the Jurassic sediments has been noted (exploration well 204/17- 1). Late Sequence T40 (unit F1b) is defined by the dinocyst *Apectodinium A. Augustum* that is diagnostic of the Palaeocene to Eocene transition (Thomas & Shackleton, 1996). This dinocyst is ubiquitous to the F1b interval

appearing in wells from the Corona Basin (exploration well 213/23- 1) to the condensed Flett sequences off the Judd High (exploration well 204/27a- 1).

Upper Flett Formation (Ypresian 55.2–54.9 Ma)

Sequence T45 is characterised by high amplitude reflections marking a highly variable post-volcanic succession containing frequent coals. Sequence T45 is more widely distributed than the underlying Sequence T40 succession as the incised drainage network was infilled (Fig. 2) (Ebdon *et al.,* 1995) although it pinches out towards basin highs such as the Rona Ridge and Solan Bank High. The base of Sequence T45 is marked by a maximum flooding surface contained within the Colsay 1 intra-basaltic sequence on the Corona Ridge (e.g. discovery well 213/27- 1) (Schofield & Jolley, 2013).

The base of the Sequence T45 Flett Formation is marked by an influx of diverse palynoflora and woody debris (e.g. exploration wells 204/14- 2 and 204/17- 1) including the frequent occurrence of *Caryapollenites veripites* and *Triatriopollenites subtriangulus* (Jolley, 2009) (exploration wells 6005/15-1 and 6004/12- 1). Throughout deposition of the lower Sequence T45 (unit F2) eruption of the Faroe-Islands Basalt Group was still ongoing. Volcanic rocks of this age are identified on the Corona Ridge (Schofield & Jolley, 2013) and in the Corona Basin (exploration well 6005/15- 1) within which common *Caryapollenites inelegans* has been identified as Sequence T45 Flett Formation (upper F2) (Jolley, 2009). This specimen is also identified within the Malinstindur Formation interbeds on the Faroe Islands (Passey & Jolley, 2008). The upper Sequence T45 Flett Formation (unit F3) is identified by the influx of *Cerodinium wardenense.* This dinocyst is recorded throughout the Faroe-Shetland region (Jolley, 2009).

The Sequence T45, base F3 Flett Formation was mapped as a strong, continuous, negative reflector throughout much of the study area (Fig. 4A). During this time, the palaeo-

coastline was positioned over the Cambo High where Sequence T45 shoreface sands have been encountered (discovery well, 204/10- 1) (Fielding et al., 2014) alongside notable strand plains. Further south of the palaeocoastline, the sequence becomes increasingly heterogenous with a high abundance of coals, particularly around the Westray High (e.g. exploration well 204/13- 1). In the Corona Basin, the base F3 horizon directly overlies the top of the T45 volcanics in the area (exploration well 6005/15- 1). These appear as a low variance, high amplitude feature towards the north (Fig. 4A). In the Foinaven Sub-Basin, west of the Westray Ridge, dendritic drainage that formed synchronous to T38-T40 uplift has not been completely infilled by Sequence T40 to base Sequence T45, F2 sediments (Fig. 4A). Fluvial sequences sourced from the largest of these valleys are clearly imaged in the northern Foinaven Sub-Basin (exploration well 6004/12- 1).

Balder Formation (Ypresian 54.9–54.3 Ma)

Sequence T50 in the Faroe-Shetland Basin can be separated into the Balder Tuff Formation and a non-tuffaceous Balder Formation found predominantly south of the palaeo-coastline (Watson *et al.,* 2017) (Fig. 3). The Balder Tuff Formation is an important stratigraphic and seismic marker. Tuffaceous lithologies in the Faroe-Shetland Basin are best preserved in claystone lithologies on the inner to outer neritic shelf below the palaeo-wave base, north of the palaeocoastline. Outside the area where the Balder Tuff was deposited, the base of the Sequence T50 Balder Formation is defined by a maximum flooding event with high amplitude reflectors in the Judd and Foinaven Sub-basins that are indicative of coals (Ebdon *et al.,* 1995). To the south, the Sequence T50 Balder Formation lies unconformably atop the T38/T40 uplift event. The coastline by base Sequence T50 is well defined, marked by the abrupt change in RMS amplitude just south of the Cambo High with minor retreat of the coastline of ~ 6 km relative to the Sequence T45 base F3 Flett Formation (Fig. 4B). Palynologically, the base of

253 Sequence T50 is marked by abundant terrestrially derived miospores such as *Caryapollenites*
254 *circulus* and *Inapaturopellnites spp.* (Jolley, 2009). Where marine influxes occur, rare records of
255 *Coscinodscus sp. 1, Deflandrea oebisfeldensis* and *Ceratiopsis wardensis* are recorded (e.g. the
256 Corona Basin, exploration well 6005/15- 1) (Ebdon *et al.,* 1995; Jolley, 2009).

257 The upper Sequence T50 Beauly/Balder Formation coastline is demarked by the
258 presence of the Balder Tuff (Fig. 4C). Preservation of tuffaceous lithologies in the Sequence
259 T50 Balder Tuff member are marked by a bright, continuous negative reflector throughout
260 much of the Flett Basin. Notably, the Sequence T50 palaeocoastline for the Balder Tuff shows
261 ~14 km of retreat towards the south west relative to the underlying base Sequence T50
262 coastline (Fig. 4C). Deposition of the Sequence T50 Beauly Formation was extensive over the
263 area south of the palaeocoastline. The dendritic drainage in the Foinaven and Judd Sub-Basins
264 was almost submerged by this time and a retreat of the location of coals southward relative
265 to Sequence T45 is indicative of retreat of the coastline (exploration well 204/17- 1).
266 Elsewhere, Sequence T50 Beauly Formation sediments directly overlie the T38-T40
267 unconformity. In these sequences, dendritic drainage owing to the uplift of the basin is still
268 visible (Fig. 4C).

269

270 **Lower Horda Formation (Ypressian 54.3–53 Ma)**

271 Throughout the southern Faroe-Shetland Basin, lower Horda Formation sediments are
272 dominated by coastal to shallow-marine deposits (Boldreel & Andersen, 1993). To the north,
273 the palaeo-water level deepens quickly into outer shelf facies in the centre of the basin (Fig.
274 4C). Jolley. (2009) noted a palynoflora assemblage of *Caryapollenites veripites* (frequent) and
275 *Thomsonipollis magnificoides* as being indicative of the lower Horda Formation. The base of the
276 Horda Formation is also noted as exhibiting a major radiolarian spike with frequently abundant
277 *Cenosphaera spp*.. Landward migration of the coastline continued throughout the lower Horda

Formation (Fig 4C). Here, bright and heterogenous horizons indicative of shelf sands, muds and coastal plains are confined ~80 km (Fig. 4C) to the southwest showing significant coastline retreat relative to the Balder Formation.

UNEARTHING THE AGE AND LOCATION OF PALAEOCOASTLINES

Age constraints determined for the Faroe-Islands Basalt Group have provided a geochemical basis with which to correlate with the related sedimentary sequences in the Faroe-Shetland Basin. In particular, radiometric ages (Tarling & Gale, 1968; Waagstein *et al.,* 2002) and the geomagnetic polarity timescale (Cande & Kent, 1995) have been used alongside seismic reflection data, wireline logs and biostratigraphical correlations to tie together the offshore and onshore sequences (Ellis *et al.,* 2002; Schofield and Jolley, 2013). In combination with regional biostratigraphy, the identification of global biostratigraphical events have tied the sequences in the Faroe-Shetland Basin to the geological timescale of Gradstein *et al.,* 2004 (Jolley & Bell, 2002; Jolley, 2009). In order to provide an approximate age for the mapped coastlines, the seismic horizons were tied to the available wells and a relative age based on the aforementioned techniques was assigned (Fig. 3 and Fig. 6).

To estimate the rate of subsidence throughout the post-volcanic succession, a time to depth conversion of the mapped horizons was undertaken using the 11 wells that were identified as having vertical seismic profile data throughout the Upper Palaeocene to Lower Eocene succession (Fig. 6). Following depth conversion, the location of the palaeocoastlines was overlain on top of the depth converted horizons, to constrain the present day depth of the palaeocoastlines within the subsurface (Fig. 6). The change in depth of the palaeocoastlines was then taken as an approximation for the relative amount of sediment deposited between each successive palaeocoastline and, hence, the relative amount of subsidence that had occurred between each palaeocoastline.

303 The effects of sedimentary compaction were removed by undertaking three 1D
304 studies on wells adjacent to the successive palaeocoastlines. We chose to undertake a 1D
305 decompaction for the successive positions of the coastline at 54.9, 54.5 and 54 Ma using the
306 technique outlined in Allen & Allen (2013). Considering a layer of sediment at present day
307 depths of y1 and y2, which was then moved vertically to shallower depths of y'1 and y'2, the
308 general decompaction equation is:

309 $$y'_2 - y'_1 = y_2 - y_1 - \frac{\emptyset_0}{c}\{\exp(-cy_1) - \exp(-cy_2)\} + \frac{\emptyset_0}{c}\{\exp(-cy'_1) - \exp(-cy'_2)\}$$

310 Where $\emptyset_0$ is the initial porosity and c is a coefficient that determines the slope of the porosity
311 depth curve for a given lithology. We chose three wells within the study area that were
312 positioned at, or near, the palaeocoastline during the times of interest to give the most
313 accurate result: exploration well 204/10a- 3 for 54.9 Ma; exploration well 6004/12- 1 for 54.5
314 Ma and exploration well 204/27a- 1 for 54 Ma. The values used for decompaction from these
315 wells are displayed in Fig. 7. Given that the overburden is relatively homogenous, and only
316 large scale relative changes in depth were of interest, the overburden was approximated to
317 be that of either a silty sandstone or a sandstone based on the petrophysical response.
318 The general decompaction equation was then solved through Newton-Raphson iteration,
319 providing decompacted thicknesses (y'_2) of:

320 A. 204/10a- 3. Present day thickness = 1330 m. 54.9 Ma = 1674 m
321 B. 6004/12- 1. Present day thickness = 1140 m. 54.5 Ma = 1386 m
322 C. 204/27a- 1. Present day thickness = 865 m. 54 Ma = 1003 m

323 Figure 7 shows the columns of sediment that were subject to depth conversion,
324 decompaction and then used to constrain the magnitude of subsidence between 54.9-54 Ma.
325 These calculations were subject to errors in the decompaction of the columns of the sediment
326 in addition to the resolution of the seismic data used to locate the palaeocoastline. The main

errors include the vertical resolution of the seismic data (±23 m, giving a maximum error of 2.5%) and changes in porosity with depth (estimated at ±10%, after Shaw Champion *et al.*, 2008). In depth converting the horizons, Figure 6F shows the maximum and minimum time depth curves resulting in a ±10% error in depth conversion of the horizons, highlighted in the longitudinal position of the palaeocoastline (Figure 8). Errors in the age dating of the horizons are attributed to the biostratigraphical zonation of the Faroe-Shetland Basin. The biostratigraphy of the Palaeocene and Eocene of Faroe-Shetland Basin is well defined, with maximum errors of ±0.25 Ma for the succession between 55.4 Ma and 54 Ma (Jolley, 2009).

Notably, throughout the depth conversion and decompaction of the palaeocoastlines we have not taken into account the elastic thickness of the lithosphere. As was noted in Clift & Turner (1998), the lithosphere beneath extensional sedimentary basins during rifting is relatively weak (e.g. the North Sea, Barton & Wood, 1984) and especially weak in uplifted and severely faulted regions, such as East Africa (Ebinger *et al.*, 1989). Additionally, despite widespread evidence for Oligocene to Miocene aged inversion throughout the Faroe-Shetland basin (Boldreel & Andersen, 1993) the lack of significant uplift of the basin during this time is further evidence in support of a low elastic thickness in the Faroe-Shetland Basin. Due to the significant evidence in favour of a low elastic thickness, we have therefore assumed local isostatic compensation of the lithosphere and an effective elastic thickness of zero, similar to Clift & Turner (1998).

DISCUSSION

Factors Effecting Measurements of Subsidence and Coastline Retreat

Three key factors exist that may have contributed to the observed amount of subsidence within the Faroe-Shetland Basin that must be discussed before we can focus on the dynamic component of Eocene subsidence:

- Eocene extension in the Faroe-Shetland Basin (e.g. Dean *et al.*, 1999).
- Oligocene to Miocene aged inversion of the Faroe-Shetland basin (Boldreel & Andersen, 1993).
- Eustatic changes in sea level.

Eocene-aged extension has been noted by previous authors such as Mudge & Rashid (1987) and Dean *et al.* (1999). Where extension is noted, it occurs predominantly within the Flett Basin, north east of the extent of the study area. Additionally, there is fault controlled thickening observable in the T60 sediments of the Flett Basin, lending credence to a phase of fault growth synchronous with subsidence in the Flett Basin (Mudge & Rashid, 1987; Dean *et al.* 1999). However, throughout the Judd and Foinaven Sub-basins where the study is located, Eocene age faulting has not been noted. Notably, the stratigraphic link between the Balder Formation and enhanced subsidence in the Faroe-Shetland Basin is an indication that rifting had initiated further west, at the site of future sea floor spreading (Dore *et al.*, 1999). As such, we argue that Eocene subsidence within the Faroe-Shetland Basin was not due to active extension within the Faroe-Shetland Basin, although some element of extension was undoubtedly present. It is deemed more likely that dynamic subsidence in the Eocene facilitated reactivation of major basement bounding faults in the Faroe-Shetland Basin.

More significant is the effect that Oligocene-Miocene latter-day compression and inversion in the North Atlantic (Dore *et al.*, 1999) had on the Faroe-Shetland Basin. In particular, subsequent deformation of the palaeocoastlines observed in certain areas. Throughout the end of the Eocene and spanning the Oligocene to mid-Miocene, the Faroe-Shetland Basin was subject to a compressive regime, resulting in inversion of the main ridges and structural highs (Ritchie *et al.*, 2008). The effects of inversion on the depth of palaeocoastlines were investigated by measuring the depth of the palaeo-coastlines at 5 km intervals across the study area (Fig. 8). These depths were then superimposed on the two

377 way travel time map of the base Cretaceous (see Fig. 1) to mark the sections of the coastline
378 that lay directly on top of basin highs, such as the Cambo and Westray. Notably, there is an
379 abrupt change of up to 200 m in the depth of the palaeocoastlines in areas overlying basin
380 highs. Clearly there is uncertainty in determining how much the present day depth of the
381 palaeocoastlines has been effected by inversion. Importantly, only areas away from these
382 structural highs were analysed when calculating changes in depth and position of the
383 paleocoastlines. Although the sub-basins have undoubtedly also experienced some
384 compression during the Oligocene and Miocene, the coastlines measured were all contained
385 within the Judd and Foinaven Sub-Basins. As these basins are broadly contiguous, it was
386 assumed that they have remained within a similar tectonic regime since deposition.

387 Critically, the methodology used within this paper, which measures the relative
388 changes between seperate palaeocoastlines, means that later tectonic events or inversion
389 would not have had a major impact on the findings of the paper. This outcome is reaffirmed
390 by the similarity in the amount of subsidence measured to the amount of uplift determined by
391 previous authors (Shaw Champion *et al.*, 2008; Hartley *et al.*, 2011), who did not quantify
392 potential inversion.

393 Finally, eustatic changes occur on the order of ~150 metres in the Cenozoic (Haq *et*
394 *al.*, 1987). As noted, ~0.5 – 1 km of subsidence throughout the Late Palaeocene and Early
395 Eocene (marked by retreat of the palaeocoastline), and therefore eustasy cannot account for
396 the scale and rapidity of the subsidence observed in the Faroe-Shetland Basin. Additionally,
397 the magnitude of uplift and subsidence observed within the Faroe-Shetland Basin is localised,
398 as uplift of a similar age on the East Shetland Platform (300 km east of the study area) is of a
399 lesser extent, with much less incision of the Palaeolandscape at peak uplift (Underhill, 2001;
400 Stucky de Quay *et al.*, 2017). As eustatic changes in sea level are global, they cannot account

401 for the uplift and subsidence observed across the Faroe-Shetland Basin and East Shetland
402 Platform
403
404 **Long-Lived Dynamic Support of the Faroe-Shetland Region**
405 The coincidence of the Faroe-Islands Basalt Group, the base Flett uplift event and the post-
406 volcanic stratigraphy have led authors to attribute rapid subsidence in the Eocene succession
407 to a decrease in the dynamic support of an early Eocene mantle plume in the Northeast
408 Atlantic (Nadin *et al.*, 1997; Clift & Turner, 1998; Shaw Champion, 2008). Many of these
409 studies have focused on the use of backstripping (Hall & White, 1994, sequence stratigraphy
410 (Jones & Milton, 1994) and palaeobathymetry (Bertram & Milton, 1989; Nadin *et al.*, 1997),
411 however, more recently 3D seismic data has been used to constrain vertical motions within
412 the Faroe-Shetland Basin. Hartley *et al.* (2011), mapped the base Flett uplift unconformity
413 throughout the southern Faroe-Shetland Basin. Drainage patterns were reconstructed by
414 calculating the flow directions on the unconformity, revealing eight tributaries on the
415 palaeolandscape. To reconstruct the uplift history, Hartley et al. 2011 used longitudinal
416 profiles of the tributaries to calculate the uplift rate as a function of time (see Fig. 9A). We
417 also compare our study to that done by Shaw Champion *et al.* (2008) (Fig. 9A). Shaw
418 Champion *et al.* (2008) used a summit envelope (a smooth surface joining local maxima on a
419 topographic surface) to calculate the vertical relief on the unconformity surface. From this
420 relief, the decompacted depositional thickness of the different formations was used to
421 estimate subsidence. The study presented here is the first time 3D palaeogeographical
422 features (in this case, the migrating palaeocoastline) have been used to constrain subsidence
423 throughout the early Eocene of the Faroe-Shetland Basin, providing an additional constraint
424 to Late Paleocene and Early Eocene subsidence in the Faroe-Shetland Basin.

425 Within this study, we have calculated the decompacted depth of successive
426 palaeocoastlines between 54.9 and 54 Ma throughout the early Eocene of the Faroe-Shetland
427 Basin. The use of biostratigraphy has facilitated assigning an approximate age to the
428 palaeocoastlines. Here, we use the decompacted depths from the three 1D studies of wells
429 adjacent to the palaeocoastline and use the change in age and depth as a direct approximation
430 of subsidence rate. It is noteworthy that, within this study, we did not attempt to measure
431 the amount and of uplift within the Faroe-Shetland Basin during this time. Instead, we compare
432 the amount of subsidence measured within this study with previous author's measured uplift
433 (Shaw Champion *et al.* 2008; Hartley *et al.*, 2011). Shaw Champion *et al.'s* (2008) study area
434 focused on the Judd Basin and, hence, the Flett Formation sediments infilling the incised
435 drainage network. However, the presence of older Flett Formation sediments preserved
436 north of the Judd basin is well documented (Jolley, 2009; Schofield & Jolley, 2013). As Shaw
437 Champion *et al.*'s (2008) study focused on the thickness of Flett Formation sediment in order
438 to quantify the amount of uplift, it is likely their peak uplift measurement of ~550 m is an
439 underestimate. Hartley *et al.'s* (2011) river profile analysis was conducted independent of
440 sediment thickness and as Hartley *et al*'s (2011) proposed ~0.9 km of uplift closely matches
441 the total quantity of subsidence measured within this study, we recognise this value as a better
442 approximation of total peak uplift. However, unlike Hartley *et al.*, 2011, Shaw Champion et al.
443 (2008) directly measured the amount of subsidence within the Judd Basin during the Upper
444 Flett Formation, providing an approximation of subsidence rate immediately following uplift,
445 prior to 54.9 Ma. For this reason, in Fig 9A, we choose to plot an amalgamation of Hartley *et*
446 *al.'s* (2011) uplift curve and Shaw Champion *et al.*'s (2008) initial rate of subsidence, recognising
447 the strengths in both studies.
448 We find initial subsidence appears to be inhibited throughout the Flett Formation
449 (56.1–54.9 Ma), initially subsiding at ~330 m Ma^{-1} (Fig. 9A, prior to coastline A) (Shaw

Champion *et al.*, 2008). During this time, the coastline migrated landwards by ~20 km. However, coeval with the termination of the emplacement of the Faroe Island Basalt group and initiation of rifting in the North Atlantic, ~54.9 Ma, coastline migration accelerated throughout the Balder and lower Horda Formations, subsiding ~766m Ma^{-1} between 54.9–54 Ma (Fig 9A, coastlines A-C). Within the seismic reflection data, this is marked by rapid landward migration of the coastlines ~80 km to the south as fully marine conditions were established in the centre of the basin. The ~56.1 Ma base Flett Formation erosional surface, mapped by previous studies has been attributed to thermal uplift related to the impingement of the Icelandic hotspot in the region (Nadin *et al.*, 1997; Hartley *et al.*, 2011).

Our estimates of subsidence throughout the Lower Eocene, 54.9–54 Ma, are of a similar magnitude (~1 km) to the scale of uplift proposed by previous studies (Rudge *et al.*, 2008; Hartley *et al.*, 2011). However, rather than noting a transient phase of uplift at 55.4 Ma immediately followed by rapid subsidence (Hartley *et al.*, 2011), our work supports previous authors (Nadin *et al.*, 1997; Clift & Turner, 1998; Smallwood & Gill, 2002; Fletcher *et al.*, 2013) who suggest that the Faroe-Shetland Basin was subject to prolonged dynamic support. We find that the Faroe-Shetland Basin does not subside rapidly until at least 0.45 Myrs after peak uplift has occurred at 55.4 Ma (Fig. 9). Our findings provide new constraints on the duration of dynamic support adjacent to the Iceland plume. Previous authors postulated that subsidence following initial phases of uplift is rapid (~2000 m Ma^{-1}) and attributable to movement of mantle thermal anomalies beneath the Faroe-Shetland Region in a west to east direction (Hartley *et al.*, 2011; Stucky de Quay *et al.*, 2017) (Fig. 9A). The model of movement of this mantle thermal anomaly, and proposed synchronous uplift, has been applied to the concurrent Bressay Unconformity on the East Shetland Platform of the North Sea (White, 1997; Stucky de Quay *et al.*, 2017), which experienced uplift and erosion between 58–55 Ma (Stucky de Quay *et al.*, 2017). However, our finding of 2 Myrs of dynamic support and delayed accelerated subsidence

475 contrasts with the findings of Hartley *et al.* and Stucky de Quay *et al.* (2011, 2017), who
476 conclude that both rapid uplift and subsidence occurred 58–55 Ma. We thus find transient
477 uplift due to the movement of hot plume annulus difficult to reconcile with the sedimentary
478 stratigraphic record of subsidence, as it does not account for the inhibited subsidence
479 following uplift that may also be recorded on the East Shetland Platform.

480 The impingement of a rising plume of hot mantle has been shown to generate uplift
481 through a number of distinct mechanisms (White & McKenzie, 1989; Sleep, 1990). For the 2
482 Ma timescale proposed here, we consider two main mechanisms that could have generated
483 anomalous subsidence, following uplift, in the Upper Palaeocene/Lower Eocene of the Faroe-
484 Shetland Basin:

485 1. Localised uplift due to the thermal effects of the Iceland Plume
486 2. Regional uplift due to the magma-flow field of the ascending plume (e.g.
487 Courtney & White, 1986)

488 The thermal effect of the Iceland Plume, is recognised at present day Iceland, where the seabed
489 is anomalously shallow by 2 km. This decreases towards Scotland, where the present day
490 dynamic support is estimated to be ~500 m (Davis *et al.*, 2012). Changes in dynamic support
491 of this scale are accounted for by a thermal anomaly of 150°C across the North Atlantic (Clift,
492 1997; Schoonman *et al.*, 2017). However, thermal changes in the Iceland Plume at ~54.9 Ma
493 are more difficult to quantify. Tegner *et al.* (1998) note cooling of the Iceland Plume recorded
494 in flood basalts erupted on Greenland at ~55.5 Ma. Similarly, Spice *et al.* (2016) summarised
495 geochemical data to conclude that, initially, the Iceland Plume was associated with a pulse of
496 anomalous hot mantle over a large area (~ 2000 km) followed by a reduction in temperature
497 perhaps associated with narrowing of the plume head. Similar thermal changes of the Iceland
498 plume are noted by the earliest v-shaped ridges in the proximity of Iceland (Parnell-Turner *et*
499 *al.*, 2014). Concurrent to the initiation of rapid coastline retreat in the Faroe-Shetland basin

500 described in this paper, Tp calculated from residual depth profiles of v shaped ridges at that
501 time, show an overall cooling trend (Parnell-Turner *et al.*, 2014). However, how pronounced
502 of a thermal effect existed across the North Atlantic and, in particular, the Faroe-Shetland
503 Basin is contested. Despite an early decrease in the temperature of the Iceland Plume, Clift
504 (1997) and Parnell-Turner *et al.* (2014) noted an increase in the thermal input of the Iceland
505 Plume into the North Atlantic ~40 Ma. The lack of any major unconformity in the Faroe-
506 Shetland Basin during this time draws into question how much of an impact a large change in
507 temperature of the Iceland Plume could have on the vertical motion Faroe-Shetland Basin at
508 56 Ma. Indeed Nadin & Kusznir (1995) note that the rapidity of the subsidence that follows
509 prolonged period of uplift in the Faroe-Shetland Basin precludes a mechanism involving cooling
510 of the asthenosphere or lithosphere, as this would have occurred too slowly to account for
511 the changes in subsidence rate.

512 It is therefore important to consider the impact of kinematic regional uplift due to the
513 magma-flow field of the ascending plume. Nadin & Kusznir (1995) suggested that the initiation
514 of rifting in the North Atlantic focused asthenospheric flow of the plume into the incipient rift
515 reducing the quantity of asthenosphere flowing outward and across the North Atlantic, at
516 ~54.5 Ma (Fig. 9C). In turn, this reduction in outer asthenospheric flow would have caused a
517 reduction in the dynamic support in areas adjacent to the nascent rift, such as the Faroe-
518 Shetland basin, resulting in subsidence (Fig. 9D). Although it is beyond the scope of this study
519 to attempt to quantify the relative contributions of thermal and kinematic uplift, if the thermal
520 effect was low, as has been suggested, the kinematic effect provides a compelling mechanism
521 for uplift and subsequent subsidence of the Faroe-Shetland Basin in the Early Eocene.

522 We therefore argue that, following extensive flood volcanism, dynamic support of the
523 Faroe-Shetland Basin by the Iceland plume continued (Fig. 9B). The duration (~1 Ma) of this
524 period of inhibited subsidence suggests that uplift beneath the broader North East Atlantic

lithosphere occurred over an extended period of time. However, as the incipient North East Atlantic rift opened at 55 Ma (Fig. 9C), and the crust surrounding it was thinned and weakened, uplift due to the Iceland plume became focused under the area beneath present-day Iceland (Fig. 9D). Focusing of the magma flow regime towards the locus of the incipient North Atlantic rift in conjunction with a more minor contribution from cooling of the thermal anomaly could explain a loss of dynamic support and accelerated subsidence seen at ~ 54.9 Ma, within the Faroe-Shetland Basin.

Implications for Hydrocarbon Exploration in the Southern Faroe-Shetland Basin

A prolonged period of dynamic support has notable implications for hydrocarbon exploration in the southern Faroe-Shetland Basin. This work implies that the sediment sources would have been active from T40 until late T50 (for ~ 2 Ma). Subaerial exposure and fluvial incision of the landscape is recognised in Greenland (Dam *et al.*, 1998), the Faroe-Shetland basin (Smallwood & Gill, 2002; Shaw Champion *et al.* 2008) and the North Sea (Underhill, 2001; Stucky de Quay *et al.*, 2017). Regionally, the Palaeozoic rock constituting the hinterland areas of Shetland and NW Scotland will have been subject to increased erosion and clastic production. Below, we consider the effect this more prolonged period of dynamic support would have had on the development of depocenters in the Faroe-Shetland Basin.

Within the Faroe-Shetland Basin, several discoveries situated north of the unconformity, most notably the intra-basaltic Rosebank field and the post-volcanic Cambo Field, are testament to the prospectivity of formations from this time period (Poppitt *et al., 2016*; Fielding *et al.*, 2014). A major recognised risk, however, has been reservoir presence (Schofield & Jolley, 2013). At 54.9 Ma–54.5 Ma, the coastline the Faroe-Shetland Basin is situated in the area on, or between, the Cambo High and the Westray High (Fig. 9). In order to investigate how dynamic support effected sedimentation in the area, a series of isochron

thickness maps were constructed (Fig. 10 A-C). A pronounced thickening (~100 ms) in between the Cambo and Westray Highs suggests that sediment was ponded in this area between 54.9 and 54.5 Ma (Fig. 10A). In places, the Flett Formation thins or pinches out against the Cambo and Westray Highs, opening up the possibility of a stratigraphic play in the area. Latterly, following loss of dynamic support, the area is blanketed by claystones of the Sequence T60 Horda Formation as thermal subsidence prevails (Fig. 10C), forming a potential widespread seal.

It has been noted that, in the Judd basin, too much sand may be an issue (Varming *et al.*, 2009). A number of exploration wells drilled throughout the Faroese part of the Judd Basin show that stacked sequences of sand in the lower Palaeocene led to a lack of sealing lithologies. However, these wells typically targeted turbidite lithologies (Edbon *et al.*, 1995), not the coastal to fluvial sequences noted here. We note that there is no issue regarding lack of sealing lithologies in the Upper Palaeocene, as sandstone sequences are frequently intercalated with claystone or coaly packages (e.g. Fig. 3).

CONCLUSION

We have mapped and detailed the stratigraphy and sedimentology of the post-volcanic succession of the Faroe-Shetland Basin between 56 and 54 Ma. Mapping of paleocoastlines with reference to the Upper Palaeocene to Lower Eocene stratigraphy reveals the timing and rate of subsidence following plume related uplift. Subsidence is gradual for the ~1 Myr following emplacement of the flood basalts which we attribute to longstanding thermal support from the Iceland hotspot. This is followed by rapid subsidence over 0.5 Ma of the Faroe-Shetland Basin, suggesting a loss of dynamic support synchronous with the initiation of rifting in the North Atlantic. We conclude that high resolution stratigraphy is an important tool in recording the duration of dynamic support globally and in constraining geophysical

models of mantle dynamics. We emphasise that any proposed models of plume development or crustal dynamics in the North Atlantic (or elsewhere) must properly take into account and reconcile with the sequence stratigraphic record.

ACKNOWLEDGEMENTS

J.P.A.H. thanks the UK's Natural Environmental Research Council for the award of a PhD studentship. PGS and TGS are thanked for provision of seismic data. Interpretation was conducted on Schlumberger Petrel Software and Spectral Decomposition on FFA's Geoteric Software. Dr. Ross Parnell-Turner and Dr. John Armitage are thanked for constructive and helpful reviews that improved the manuscript. The editor Prof. Peter Clift, is thanked for excellent editorial guidance and encouragement.

REFERENCES

Allen, Philip A., and John R. Allen., 2013. *Basin analysis: Principles and application to petroleum play assessment*. John Wiley & Sons.

Barton, P. and Wood, R., 1984. Tectonic evolution of the North Sea basin: crustal stretching and subsidence. *Geophysical Journal International*, ***79***, 987-1022.

Bertram, G.T. and Milton, N.J., 1988. Reconstructing basin evolution from sedimentary thickness; the importance of palaeobathymetric control, with reference to the North Sea. *Basin Research*, ***1***, 247-257.

Boldreel, L.O. and Andersen, M.S., 1993, January. Late Paleocene to Miocene compression in the Faeroe–Rockall area. In *Geological Society, London, Petroleum Geology Conference series*, **4**, 1025-1034). Geological Society of London.

598 Braun, J. 2010. The many surface expressions of mantle dynamics. *Nature Geoscience,* **3**, 825-
599 833.

600 Brodie, J. and White, N., 1994. Sedimentary basin inversion caused by igneous underplating:
601 Northwest European continental shelf. *Geology*, ***22***, 147-150.

602 Calvès, G., Clift, P.D. and Inam, A., 2008. Anomalous subsidence on the rifted volcanic margin
603 of Pakistan: no influence from Deccan plume. *Earth and Planetary Science Letters*, ***272***, 231-239.

604 Cande, S.C. and Kent, D.V., 1995. Revised calibration of the geomagnetic polarity timescale
605 for the Late Cretaceous and Cenozoic. *Journal of Geophysical Research: Solid Earth*, ***100***, 6093-
606 6095.

607 Chambers, L.M. and Pringle, M.S., 2001. Age and duration of activity at the Isle of Mull Tertiary
608 igneous centre, Scotland, and confirmation of the existence of subchrons during Anomaly
609 26r. *Earth and Planetary Science Letters*, ***193***, 333-345.

610 Clift, P.D., 1997. Temperature anomalies under the Northeast Atlantic rifted volcanic
611 margins. *Earth and Planetary Science Letters*, ***146***, 195-211.

612 Clift, P.D. and Turner, J., 1998. Paleogene igneous underplating and subsidence anomalies in
613 the Rockall-Faeroe-Shetland area. *Marine and Petroleum Geology*, ***15***, 223-243.

614 Courtney, R.C. and White, R.S., 1986. Anomalous heat flow and geoid across the Cape Verde
615 Rise: evidence for dynamic support from a thermal plume in the mantle. *Geophysical Journal*
616 *International*, ***87***, 815-867.

617 Dam, G., Larsen, M. and Sønderholm, M., 1998. Sedimentary response to mantle plumes:
618 implications from Paleocene onshore successions, West and East Greenland. *Geology*, **26**,
619 207-210.

620 Davis, M. W., et al., 2012. Crustal structure of the British Isles and its epeirogenic
621 consequences. *Geophysical Journal International*, **190**, 705-725.

622 Day, A., Klüver, T., Söllner, W., Tabti, H. and Carlson, D., 2013. Wavefield-separation
623 methods for dual-sensor towed-streamer data. *Geophysics*, ***78***, 55-70.

624 Dean, K., McLachlan, K. and Chambers, A., 1999, January. Rifting and the development of the
625 Faeroe-Shetland Basin. In *Geological Society, London, Petroleum Geology Conference series*, **5**, 533-
626 544. Geological Society of London.

627 Van Dedem, E.J. and Verschuur, D.J., 1998. 3D surface-related multiple elimination and
628 interpolation. In *SEG Technical Program Expanded Abstracts*. Society of Exploration
629 Geophysicists. 1321-1324

630 Doré, A.G., Lundin, E.R., Fichler, C. and Olesen, O., 1997. Patterns of basement structure
631 and reactivation along the NE Atlantic margin. *Journal of the Geological Society*, **154**, 85-92.

632 Doré, A.G., Lundin, E.R., Jensen, L.N., Birkeland, Ø., Eliassen, P.E. and Fichler, C., 1999,
633 January. Principal tectonic events in the evolution of the northwest European Atlantic margin.
634 In *Geological society, london, petroleum geology conference series*, **5**, 41-61. Geological Society of
635 London.

636 Duindam, P. and Van Hoorn, B., 1987. Structural evolution of the West Shetland continental
637 margin. *Petroleum Geology of North West Europe. Graham & Trotman, London*, **2**, 765-773.

638 Duncan, L., Helland-Hansen, D. and Dennehy, C., 2009, May. The Rosebank discovery: a new
639 play type in intra basalt reservoirs of the North Atlantic Volcanic Province. In *6th European*
640 *Production and Development Conference and Exhibition (DEVEX)*, 12-13.

641 Ebdon, C.C., Granger, P.J., Johnson, H.D. and Evans, A.M., 1995. Early Tertiary evolution and
642 sequence stratigraphy of the Faeroe-Shetland Basin: implications for hydrocarbon
643 prospectivity. *Geological Society, London, Special Publications*, ***90***, 51-69.

644 Ebinger, C.J., Bechtel, T.D., Forsyth, D.W. and Bowin, C.O., 1989. Effective elastic plate
645 thickness beneath the East African and Afar plateaus and dynamic compensation of the
646 uplifts. *Journal of Geophysical Research: Solid Earth*, **94**, 2883-2901.

647 Ellis, D., Bell, B.R., Jolley, D.W. and O'Callaghan, M., 2002. The stratigraphy, environment of
648 eruption and age of the Faroes Lava Group, NE Atlantic Ocean. *Geological Society, London,*
649 *Special Publications*, **197**, 253-269.

650 Ellis, D., Jolley, D.W., Passey, S.R. & Bell, B.R. 2009. Transfer zones: The application of new
651 geological information from the Faroe Islands applied to the offshore exploration of intra
652 basalt and sub-basalt strata. *In: Varming, T. & Ziska, H. (eds) Faroe Islands Exploration Conference:*
653 *Proceedings of the 2nd Conference. Annals Societatis Scientiarum Faerensis, Supplementum*, **50**,
654 205–226.

655 Fielding, K.D., Burnett, D., Crabtree, N.J., Ladegaard, H. and Lawton, L.C., 2014. Exploration
656 and appraisal of a 120 km2 four-way dip closure: what could possibly go wrong? *Geological*
657 *Society, London, Special Publications*, ***397***, 145-162.

658 Fletcher, R., Kusznir, N., Roberts, A. and Hunsdale, R., 2013. The formation of a failed
659 continental breakup basin: The Cenozoic development of the Faroe-Shetland Basin. *Basin*
660 *Research*, ***25***, 532-553.

661 Ganerød, M., Smethurst, M.A., Torsvik, T.H., Prestvik, T., Rousse, S., McKenna, C., Van
662 Hinsbergen, D.J.J. and Hendriks, B.W.H., 2010. The North Atlantic Igneous Province

663 reconstructed and its relation to the plume generation zone: the Antrim Lava Group
664 revisited. *Geophysical Journal International*, **182**, 183-202.

665 Gradstein, F.M., Ogg, J.G., Smith, A.G., Bleeker, W. and Lourens, L.J., 2004. A new geologic
666 time scale, with special reference to Precambrian and Neogene. *Episodes*, **27**, 83-100.

667 Hall, B.D. and White, N., 1994. Origin of anomalous Tertiary subsidence adjacent to North
668 Atlantic continental margins. *Marine and Petroleum Geology*, **11**, 702-714.

669 Haq, Bilal U., Jan Hardenbol, and Peter R. Vail., 1987. Chronology of fluctuating sea levels
670 since the Triassic. *Science*, **235**, 1156-1167.

671 Hartley, R.A., Roberts, G.G., White, N. and Richardson, C., 2011. Transient convective uplift
672 of an ancient buried landscape. *Nature Geoscience*, **4**, 562-565.

673 Jolley, D.W. and Bell, B.R., 2002. The evolution of the North Atlantic Igneous Province and
674 the opening of the NE Atlantic rift. *Geological Society, London, Special Publications*, ***197***, 1-13.

675 Jolley, D.W., 2009. Palynofloral evidence for the onset and cessation of eruption of the Faroe
676 Islands lava field. In *Faroe Islands Exploration Conference: Proceedings of the 2nd Conference.*
677 *Annales Societatis Scientarium Faroensis*, 149-166.

678 Jones, R.W. and Milton, N.J., 1994. Sequence development during uplift: Palaeogene
679 stratigraphy and relative sea-level history of the Outer Moray Firth, UK North Sea. *Marine*
680 *and Petroleum Geology*, **11**, 157IN1161-160IN2165.

681 Kristiansen, P., Fowler, P. and Mobley, E., 2003. Anisotropic Kirchhoff prestack time migration
682 for enhanced multicomponent imaging. In *SEG Technical Program Expanded Abstracts*. Society
683 of Exploration Geophysicists. 961-964.

684 Knox, R.W.O.B., Holloway, S., Kirby, G.A. and Baily, H.E., 1997. Stratigraphic nomenclature
685 of the UK north west margin. 2. Early Paleogene lithostratigraphy and sequence
686 stratigraphy. *British Geological Survey, Nottingham*.

687 Lamers, E. and Carmichael, S.M.M., 1999, January. The Paleocene deepwater sandstone play
688 west of Shetland. In *Geological Society, London, Petroleum Geology Conference series,* **5**, 645-659.
689 Geological Society of London.

690 Lin, A.T., Watts, A.B. and Hesselbo, S.P., 2003. Cenozoic stratigraphy and subsidence history
691 of the South China Sea margin in the Taiwan region. *Basin Research*, **15**, 453-478.

692 Nadin, P.A. and Kusznir, N.J., 1995. Palaeocene uplift and Eocene subsidence in the northern
693 North Sea Basin from 2D forward and reverse stratigraphic modelling. *Journal of the Geological*
694 *Society*, **152**, 833-848.

695 Nadin, P.A., Kusznir, N.J. and Cheadle, M.J., 1997. Early Tertiary plume uplift of the North
696 Sea and Faeroe-Shetland basins. *Earth and Planetary Science Letters*, **148**, 109-127.

697 Nøhr-Hansen, H., Sheldon, E. and Dam, G., 2002. A new biostratigraphic scheme for the
698 Paleocene onshore West Greenland and its implications for the timing of the pre-volcanic
699 evolution. *Geological Society, London, Special Publications*, **197**, 111-156.

700 Parnell-Turner, R., White, N., Henstock, T., Murton, B., Maclennan, J. and Jones, S.M., 2014.
701 A continuous 55-million-year record of transient mantle plume activity beneath
702 Iceland. *Nature Geoscience*, **7**, 914-919.

703 Partyka, Greg, James Gridley, and John Lopez., 1999. "Interpretational applications of spectral
704 decomposition in reservoir characterization." *The Leading Edge* **18.3**, 353-360.

Passey, S.R. & Jolley, D.W., 2008. A revised lithostratigraphic nomenclature for the Palaeogene Faroe Islands Basalt group, NE Atlantic Ocean. Earth and Environmental Science Transactions of the Royal Society of Edinburgh, **99**, 127-158.

Pearson, D. G., C. H. Emeleus, and S. P. Kelley., 1996. "Precise 40Ar/39Ar age for the initiation of Palaeogene volcanism in the Inner Hebrides and its regional significance." *Journal of the Geological Society,* **153.6**, 815-818.

PGS, 21/112017. "FSB2012 3D GeoStreamer®" https://www.pgs.com/data-library/europe/nw-europe/west-of-shetland/fsb2012/

Pitman, Walter C., and Manik Talwani., 1972. "Sea-floor spreading in the North Atlantic." *Geological Society of America Bulletin,* **83.3**, 619-646.

Poppitt, S., et al., 2016. "The influence of volcanic rocks on the characterization of Rosebank Field–new insights from ocean-bottom seismic data and geological analogues integrated through interpretation and modelling." *Geological Society, London, Petroleum Geology Conference series*. **8**. Geological Society of London.

Reeve, M.T., Jackson, C.A.L., Bell, R.E., Magee, C. and Bastow, I.D., 2016. The stratigraphic record of prebreakup geodynamics: Evidence from the Barrow Delta, offshore Northwest Australia. *Tectonics*, ***35***, 1935-1968.

Ritchie, J.D., Johnson, H., Quinn, M.F., Gatliff, R.W., 2008. The effects of Cenozoic compression within the Faroe-Shetland Basin and adjacent areas. Geological Society, London, Special Publications, **306**, 121–136.

Ritchie, J. D., Ziska, H., Johnson, H. & Evans, D., 2011. Geology of the Faroe-Shetland Basin and adjacent areas.

727 Rudge, J.F., Champion, M.E.S., White, N., McKenzie, D. and Lovell, B., 2008. A plume model
728 of transient diachronous uplift at the Earth's surface. Earth and Planetary Science Letters,
729 **267**, 146-160.

730 Schofield, N. and Jolley, D.W., 2013. Development of intra-basaltic lava-field drainage systems
731 within the Faroe–Shetland Basin. *Petroleum Geoscience*, **19**, 273-288.

732 Schofield, Nick, et al., 2017. "Regional magma plumbing and emplacement mechanisms of the
733 Faroe-Shetland Sill Complex: implications for magma transport and petroleum systems within
734 sedimentary basins." *Basin Research,* **29.1**, 41-63.

735 Schoonman, C. M., N. J. White, and D. Pritchard., 2017. Radial viscous fingering of hot
736 asthenosphere within the Icelandic plume beneath the North Atlantic Ocean. Earth and
737 Planetary Science Letters, **468**, 51-61.

738 Sleep, N. H., 1990, Hotspots and mantle plumes: some phenomenology: Journal of
739 Geophysical Research, **95**, 6715-6736.

740 Shaw Champion, M.E., White, N.J., Jones, S.M. and Lovell, J.P.B., 2008. Quantifying transient
741 mantle convective uplift: An example from the Faroe-Shetland basin. *Tectonics*, **27**.

742 Smallwood, J.R. and Gill, C.E., 2002. The rise and fall of the Faroe–Shetland Basin: evidence
743 from seismic mapping of the Balder Formation. *Journal of the Geological Society*, **159**, 627-630.

744 Smallwood, John R., and Jenny Maresh., 2002. "The properties, morphology and distribution
745 of igneous sills: modelling, borehole data and 3D seismic from the Faroe-Shetland
746 area." *Geological Society, London, Special Publications,* **197.1**, 271-306.

747 Spice, H.E., Fitton, J.G. and Kirstein, L.A., 2016. Temperature fluctuation of the Iceland mantle
748 plume through time. *Geochemistry, Geophysics, Geosystems*, **17**, 243-254.

749 Stucky de Quay, G., Roberts, G.G., Watson, J.S. and Jackson, C.L., 2017. Incipient mantle
750 plume evolution: Constraints from ancient landscapes buried beneath the North
751 Sea. Geochemistry, Geophysics, Geosystems, **18**, 973-993.

752 Tarling, D.H. and Gale, N.H., 1968. Isotopic dating and palaeomagnetic polarity in the Faeroe
753 Islands. *Nature*, **218**, 1043-1044.

754 Tegner, C., Lesher, C.E., Larsen, L.M. and Watt, W.S., 1998. Evidence from the rare-earth-
755 element record of mantle melting for cooling of the Tertiary Iceland plume. *Nature*, **395**, 591.

756 Tenghamn, R., Vaage, S. and Borresen, C., 2008, June. GeoStreamer, a dual-sensor towed
757 marine streamer. In *70th EAGE Conference and Exhibition incorporating SPE EUROPEC 2008*.

758 Thomas, E. and Shackleton, N.J., 1996. The Paleocene-Eocene benthic foraminiferal extinction
759 and stable isotope anomalies. *Geological Society, London, Special Publications*, **101**, 401-441.

760 Tindale, K., Newell, N., Keall, J. and Smith, N., 1998. Structural evolution and charge history of the
761 Exmouth Sub-basin, northern Carnarvon Basin, Western Australia. In *The Sedimentary Basins of*
762 *Western Australia 2: Proceedings of the Petroleum Exploration Society of Australia Symposium,*
763 *Perth* 447-472.

764 Turner, J.D. and Scrutton, R.A., 1993, January. Subsidence patterns in western margin basins:
765 evidence from the Faeroe–Shetland Basin. In *Geological Society, London, Petroleum Geology*
766 *Conference series*, **4**, 975-983. Geological Society of London.

767 Underhill, J.R., 2001. Controls on the genesis and prospectivity of Paleogene
768 palaeogeomorphic traps, East Shetland Platform, UK North Sea.. Marine and Petroleum
769 Geology, **18**, 259-281.

Van Wagoner, J.C., Posamentier, H.W., Mitchum, R.M.J., Vail, P.R., Sarg, J.F., Loutit, T.S. and Hardenbol, J., 1988. An overview of the fundamentals of sequence stratigraphy and key definitions.

Varming, T., 2009. Results from the drilling of the 1st license round wells in the Faroese part of the Judd Basin. In *Faroe Islands Exploration Conference–Proceedings of the 2nd Conference: Annales Societatis Scientarum Færoensis, Supplementum: Tórshavn, Jarðfeingi,* 346-363.

Waagstein, R., Guise, P. and Rex, D., 2002. K/Ar and 39Ar/40Ar whole-rock dating of zeolite facies metamorphosed flood basalts: the upper Paleocene basalts of the Faroe Islands, NE Atlantic. *Geological Society, London, Special Publications*, ***197***, 219-252.

Watson, D., Schofield, N., Jolley, D., Archer, S., Finlay, A.J., Mark, N., Hardman, J. and Watton, T., 2017. Stratigraphic overview of Palaeogene tuffs in the Faroe–Shetland Basin, NE Atlantic Margin. Journal of the Geological Society, **132**.

White, R. and McKenzie, D., 1989. Magmatism at rift zones: the generation of volcanic continental margins and flood basalts. *Journal of Geophysical Research: Solid Earth*, **94**, 7685-7729.

White, R.S., 1997. Rift–plume interaction in the North Atlantic. Philosophical Transactions of the Royal Society of London A: Mathematical, Physical and Engineering Sciences, **355**, 319-339.

White, Nicky, and Bryan Lovell., 1997. "Measuring the pulse of a plume with the sedimentary record." *Nature,* **387.6636,** 888.

Figures

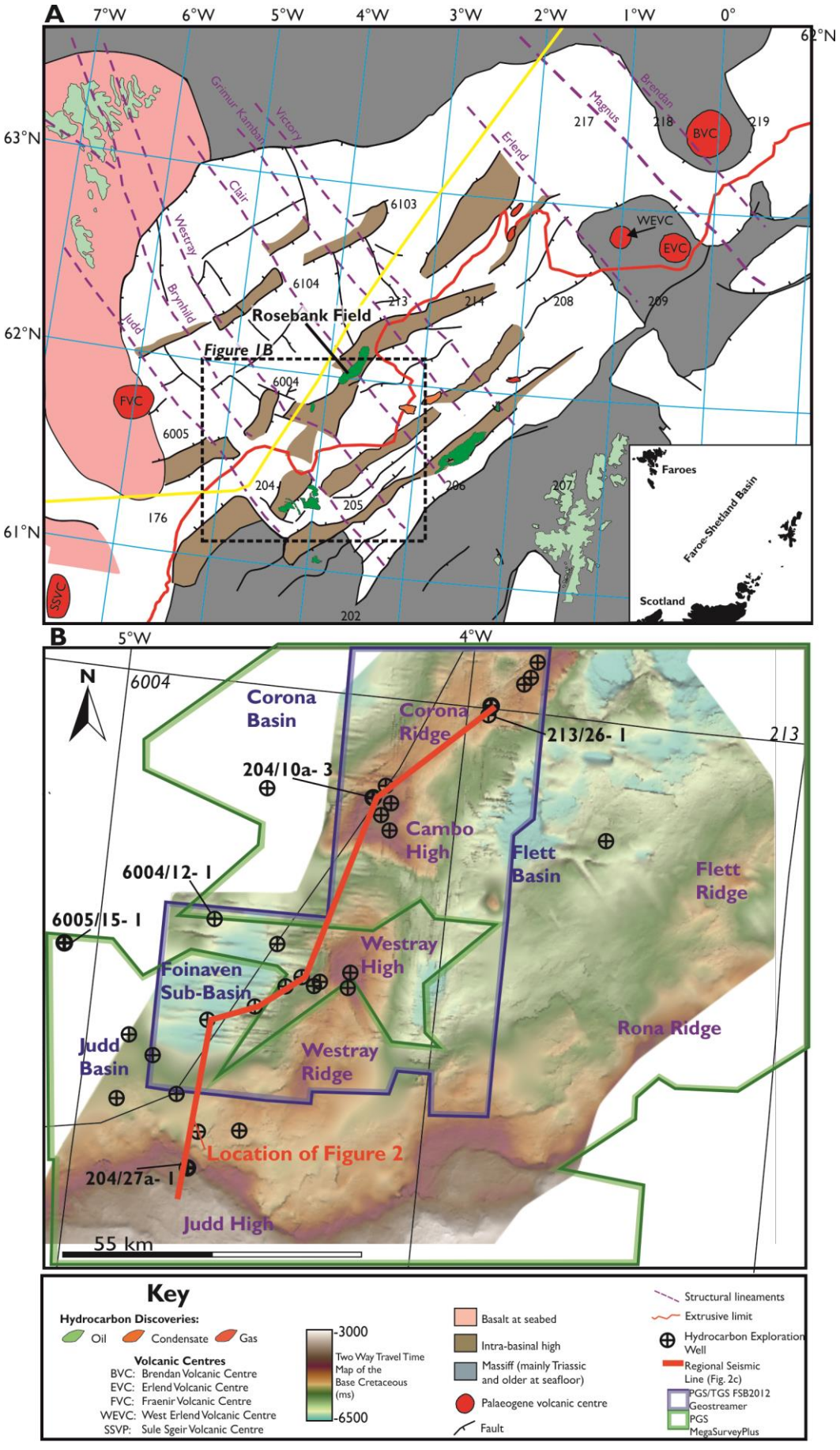
A
7°W
6°W
5°W
4°W
3°W
2°W
1°W
0°
62°N
63°N
62°N
61°N
Grinnur
Kanbar
Victory
Clair
Westray
Brynhild
Judd
Magnus
Brendan
Erlend
BVC
WEVC
EVC
FVC
SSVC
6103
6104
6004
6005
204
205
206
207
208
209
213
214
217
218
219
176
202
Rosebank Field
Figure 1B
Faroes
Faroe-Shetland Basin
Scotland
B
5°W
4°W
N
6004
213
Corona Basin
Corona Ridge
213/26- 1
204/10a- 3
Cambo High
Flett Basin
Flett Ridge
6004/12- 1
6005/15- 1
Westray High
Foinaven Sub-Basin
Rona Ridge
Judd Basin
Westray Ridge
Location of Figure 2
204/27a- 1
Judd High
55 km
Key
Hydrocarbon Discoveries:
Oil
Condensate
Gas
Volcanic Centres
BVC: Brendan Volcanic Centre
EVC: Erlend Volcanic Centre
FVC: Fraenir Volcanic Centre
WEVC: West Erlend Volcanic Centre
SSVP: Sule Sgeir Volcanic Centre
-3000
Two Way Travel Time Map of the Base Cretaceous (ms)
-6500
Basalt at seabed
Intra-basinal high
Massiff (mainly Triassic and older at seafloor)
Palaeogene volcanic centre
Fault
Structural lineaments
Extrusive limit
Hydrocarbon Exploration Well
Regional Seismic Line (Fig. 2c)
PGS/TGS FSB2012 Geostreamer
PGS MegaSurveyPlus

793

Figure 1. a, Regional structural map of the Faroe-Shetland Basin, adapted from Ellis *et al.*, 2009. Basins, highs and ridges are highlighted within the key. Lineaments are marked on the map. The location of the Rosebank Field is marked in the centre of the basin. The location of Figure 1B is marked by the inset box. **b,** Map of the study area highlighting 3D seismic data and hydrocarbon well coverage throughout the area. As part of the study, the base Cretaceous was mapped throughout the study area, highlighting the main structural highs within the study area; the Judd, Westray and Cambo Highs. The location of the seismic line in Figure 2 is also shown.

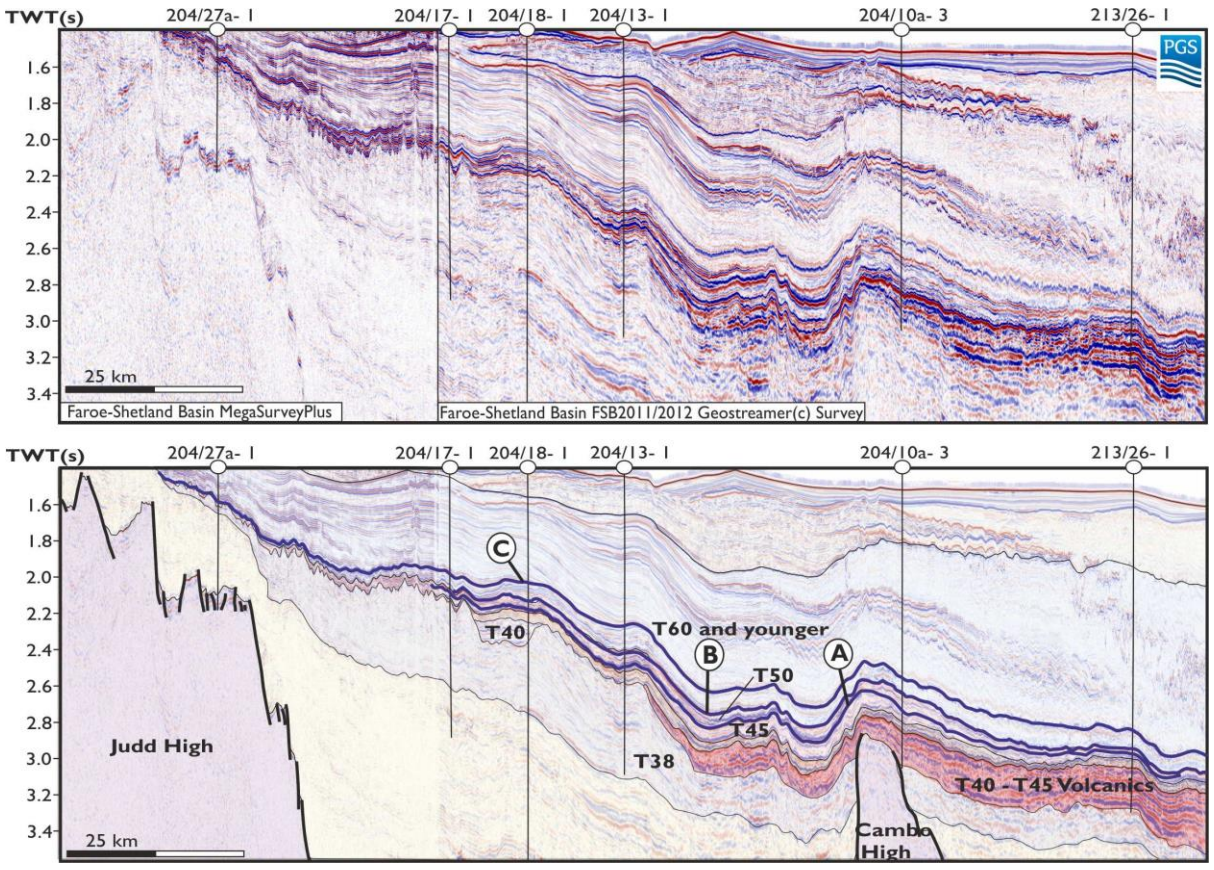

Figure 2. 2D regional seismic line running south to north through the study area. (a) Uninterpreted regional seismic line of the study area. Data courtesy of PGS (the FSB2011/12 MultiClient Geostreamer® survey and the PGS Megasurvey). (b) Interpreted regional seismc line of the study area, highlighting the Upper Palaeocene/Lower Eocene T38 – T60 succession.

Horizons mapped throughout the study area are marked by a blue line, as in Figure 3. The location of succesive palaeocoastlines is marked by A, B and C.

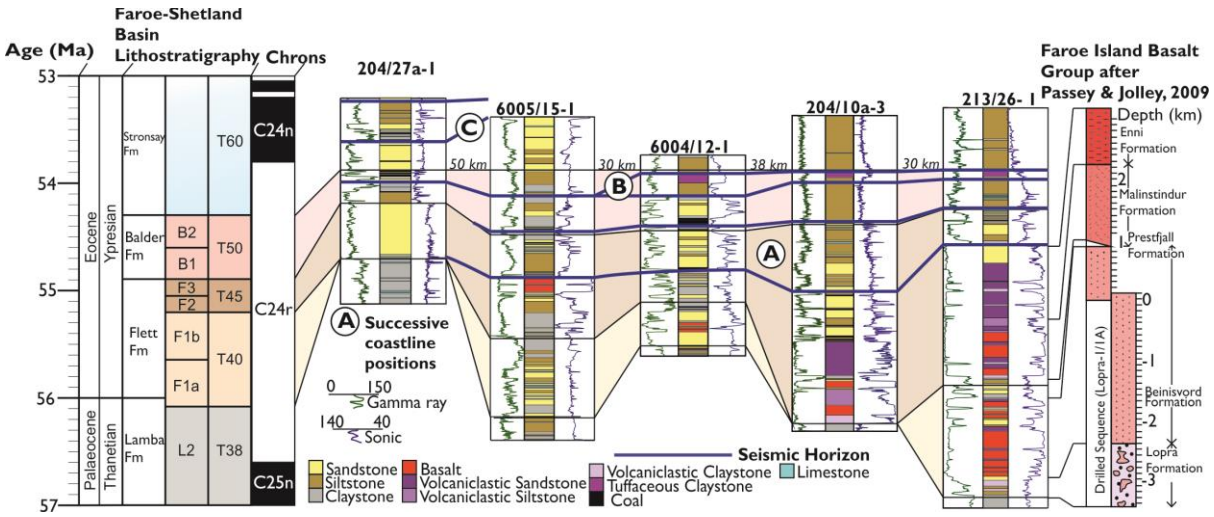

Figure 3. Stratigraphical and sedimentological overview of the study area. The age of the succesion, alongside the associated Epochs and Ages are shown to the left of the figure. This is correlated with the Faroe-Shetland Basin Lithostratigraphy taken from Ritchie (2011) and Ebdon *et al.*, 1995. Magnetic chrons are also shown to further clarify the age of the succession. To the right of the figure, the relative age of the Faroe-Islands Basalt Group is shown, after Passel & Jolley (2008). An exploration well correlation, from south to north across the study area is shown to highlight the lithological variability throughout the Late Palaeocene and Early Eocene of the Faroe-Shetland Basin. Wells were interpreted through use of petrophysical data,of which gamma and sonic are shown here.Formation tops were picked by a combination of petrophyscial response and biostratigraphic markers. The relative position of picked seismic horizons is shown by the blue lines and the successive position of the palaeocoastline is marked by A, B and C.

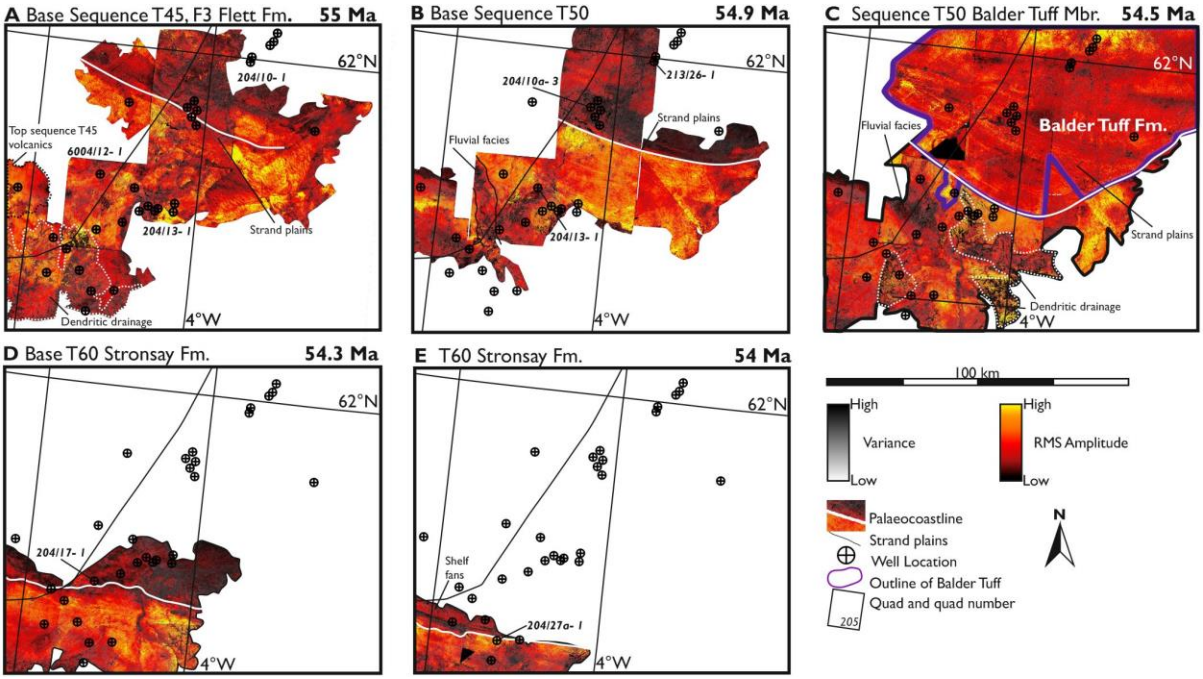

824

825 **Figure 4.** Seismic attribute maps extracted from 3D volumes along interpreted horizons
826 throughout the post-volcanic succession of the Faroe-Shetland basin. Attributes extracted
827 were variance and RMS amplitude (taken over a window of 10 ms). The transparency of the
828 low variance values was increased and all values were then superimposed on the RMS
829 amplitude volume to create an RMS ampltiude/ variance blend. Within each panel, the
830 palaeocoastline is marked by the white line on each horizon. Each panel is described in detail
831 within the text, however, note the gradual retreat of the coastline towards the south (Fig.
832 3A-C) followed by a more marked retreat observable between figures 3C and 3D.

833

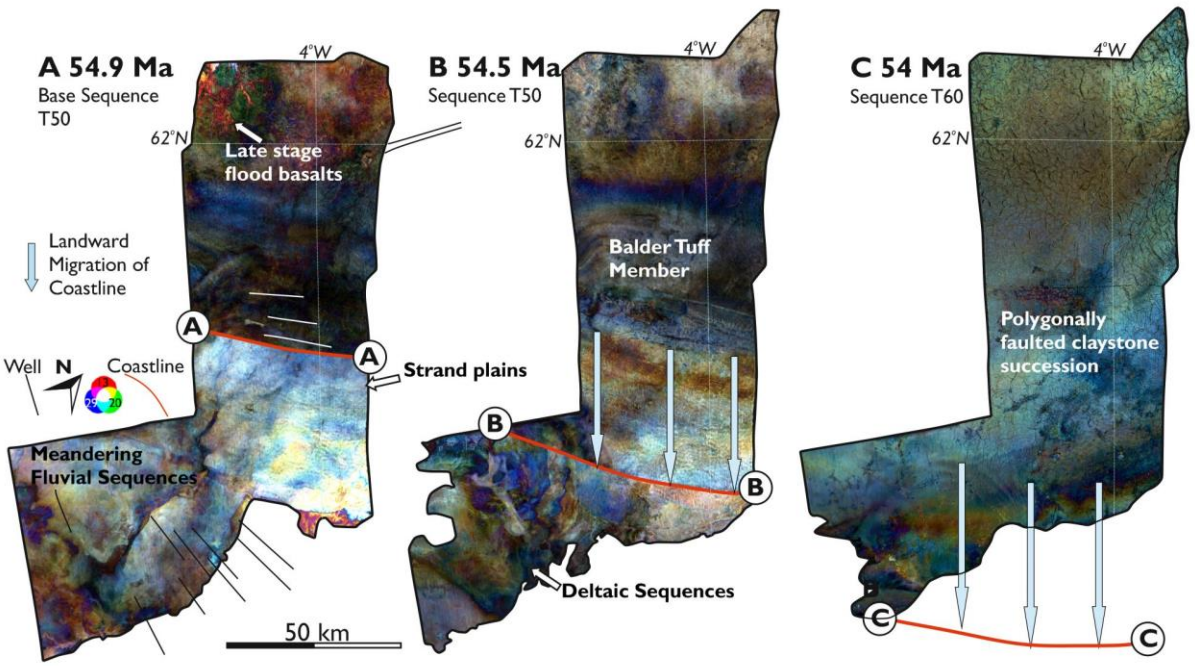

834

835 **Figure 5.** RGB frequency spectral decompositioncarried out on the select horizons mapped
836 within the Faroe-Shetland Basin 2011/12 Geostreamer© Survey. The palaeocoastline is marked
837 by the red line on each horizon. **A** The palaeocoastline is marked by a sharp change in the
838 brightness and colour of the RGB spectral decomposition of the Base Sequence T50 Horizon.
839 South of the palaeocoastline, meandering fluvial sequences are observable in the southwest of
840 the survey. **B** The palaeocoastline is marked by the southern limit of the Balder Tuff, due to
841 its preservation below the palaeo-wave base in the Faroe-Shetland Basin. The Balder Tuff
842 Member is marked by a bright negative reflector, hence the brightness of lithologies norht of
843 the palaeocoastline, relative to Fig. 5A. **C** The palaeocoastline is outside the FSB2011/12
844 Geostreamer© Survey by Sequence T60, 54 Ma. Here, the previous variance/RMS blend (Fig.
845 4) was used to constrain the exact location of the palaeocoastline. Throughout the three
846 horizons, note the gradual retreat of the coastline towards the south followed by a more
847 marked retreat observable between figures 3B and 3C.

848

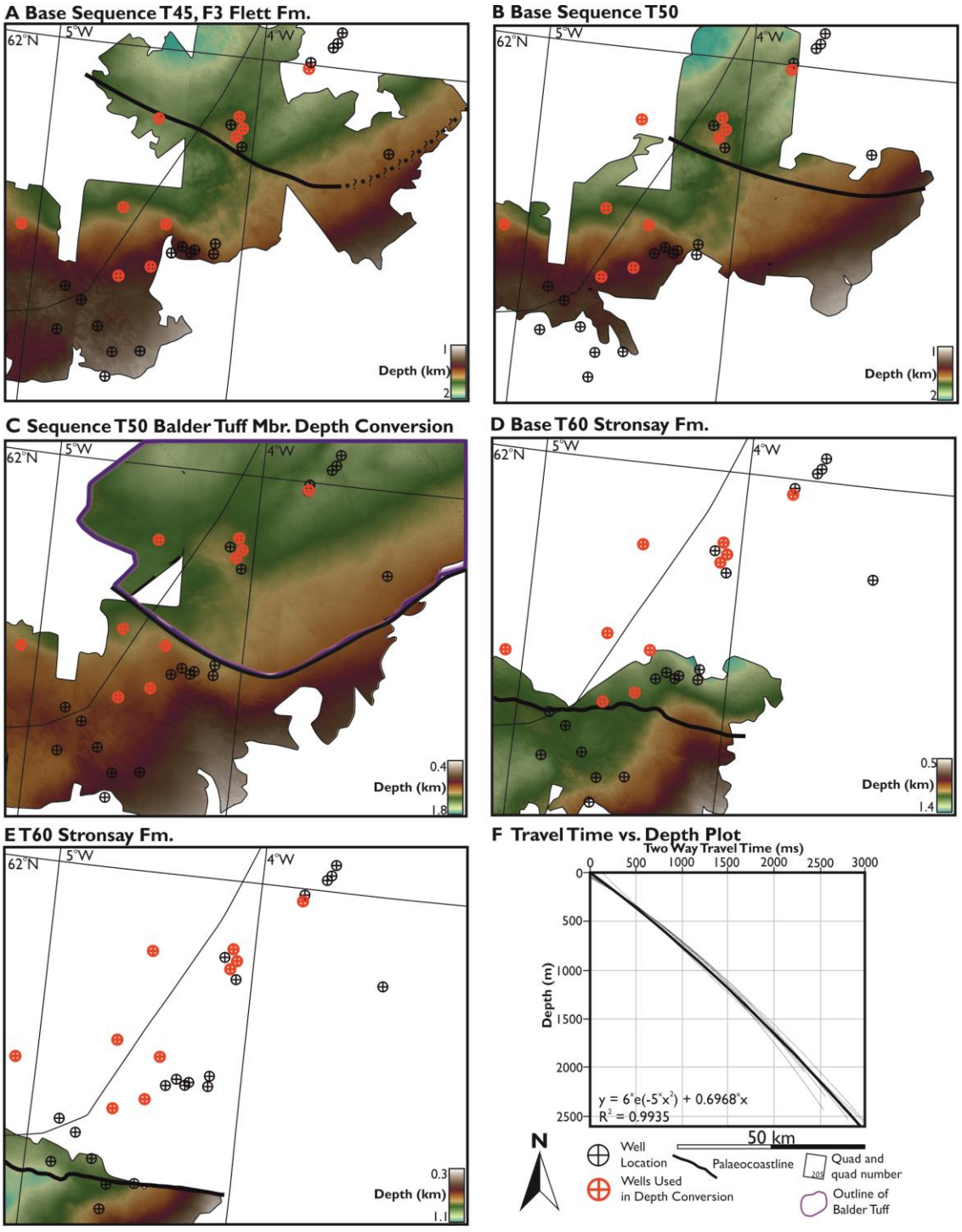

Figure 6. Depth conversion of horizons mapped throughout the study area. Of the 34 wells within the study area, 11 were found to have sufficient data (i.e. velocity/depth data throughout the Upper Palaeocene/Lower Eocene succession), while the remaining 23 wells lacked sufficient time-depth data throughout the interval studied. An average time depth relationship was calculated by plotting the VSP (Vertical Seismic Profile) data together and

855 fitting a best fit line to the data (Fig. 2F). This relationship was then used to convert the
856 horizons from time to depth (Fig. 2A-E). Red lines show best fix maximum and minimum
857 models.

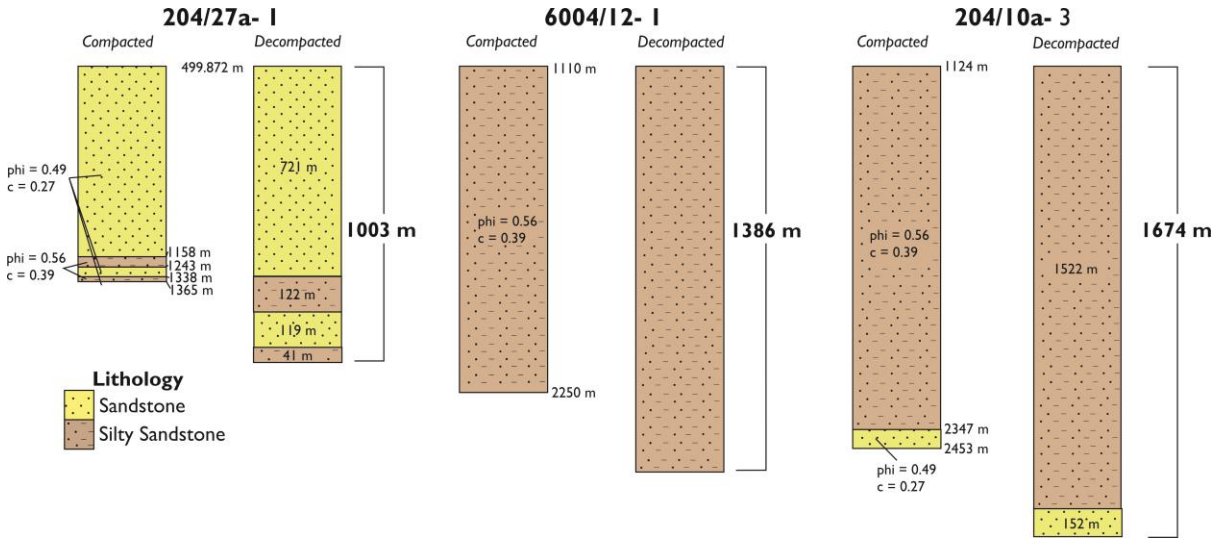

858

859 **Figure 7.** Columns of sediment used for the 1D decompaction and, adjacent to them, the
860 decompacted thicknesses. Values placed into the general decompaction equation are noted
861 on the compacted columns. Stratigraphic depths were taken from composite well logs of the
862 exploration wells studied.

863

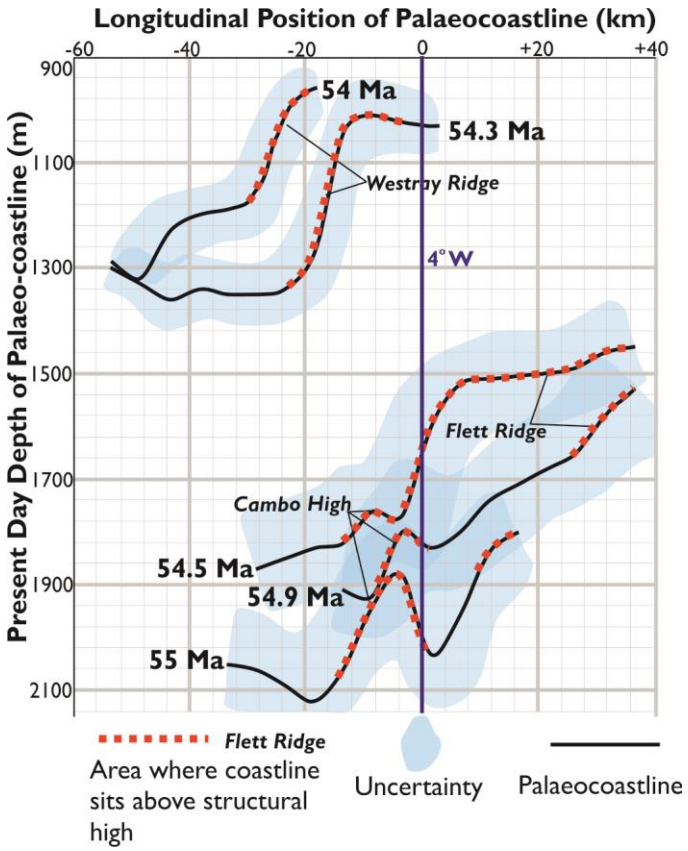

Figure 8. Depths of the palaeo-coastlines taken at 5 km intervals across the study area. X axis distances are given with respect to the longitude of 4°W, to act as a reference point on previous figures. The present day depth of the palaeocoastlines was measured on the depth converted horizons shown in Figure 6. Starting at the most western point on each horizon, the depth was measured every 5 km. The restricted nature of the palaeocoastlines is a reflection of the limits of the 3D seismic data available throughout the study.Dashed red lines denote where the palaeocoastline overlies basin highs. These basin highs were primarily identified on the 3D map of the Base Cretaceous shown in Fig 1A. The abrupt change in depth of the palaeocoastlines in these positions is a product of cenozoic inversion. As in previous figures, note the abrupt change in the depth of the palaeocoastline bwteen 54.5 ma and 54.3 Ma, synchronous with rapid retreat of the palaeocoastline towards the mainland.

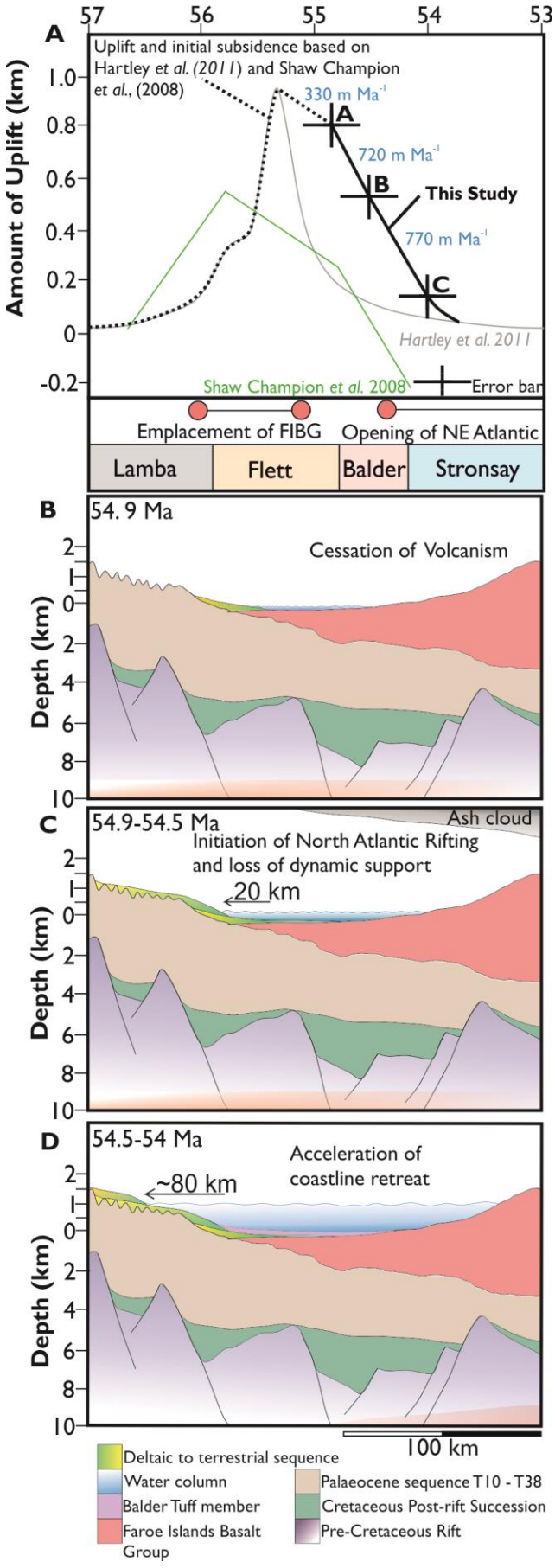
A
Uplift and initial subsidence based on Hartley et al. (2011) and Shaw Champion et al., (2008)
Amount of Uplift (km)
330 m Ma-1
720 m Ma-1
770 m Ma-1
This Study
Hartley et al. 2011
Shaw Champion et al. 2008
Error bar
Emplacement of FIBG
Opening of NE Atlantic
Lamba
Flett
Balder
Stronsay
B
54. 9 Ma
Cessation of Volcanism
Depth (km)
C
54.9-54.5 Ma
Ash cloud
Initiation of North Atlantic Rifting and loss of dynamic support
20 km
D
54.5-54 Ma
Acceleration of coastline retreat
~80 km
100 km
Deltaic to terrestrial sequence
Water column
Balder Tuff member
Faroe Islands Basalt Group
Palaeocene sequence T10 - T38
Cretaceous Post-rift Succession
Pre-Cretaceous Rift

877

878 **Figure 9. A** Observed and measured uplift and subsidence. Uplift was not measured within
879 this study, instead, we compare our proposed amount of subsidence to the uplift and
880 subsidence of Shaw Champion *et al.*'s and Hartley *et al.*'s (2008, 2011).Starting with a
881 combined curve of Hartley *et al.*'s uplift and Shaw Champion *et al.*'s initial subsidence (2008.
882 2011), as explained in the main text, we plot a proposed uplift and subsidence curve for the
883 southern Faroe-Shetland basin between 57 and 53 Ma. Data points calculated in this study
884 are denoted by the solid black line and have been derived from the decompacted 1D columns
885 of sediment and the relative change in thickness of sediment between columns A, B and C
886 respectively (Fig. 7), with reference to the present day depth of the palaeocoastlines noted
887 in Figs. 6 & 8. The size of the error bars is explained within the text. Notably, subsidence is
888 initially gradual until 54.9 Ma, at which point it occurred more rapidly. We also display three
889 idealised cross sections through the Faroe-Shetland Basin designed to illustrate the large scale
890 palaeogeographical changes observed in this study. **B** 54.9 Ma following cessation of the
891 Faroe-Islands Basalt Group. **C** 54.9-54.5 Ma. Ash cloud from the north denotes initiation of
892 volcanism from the proto north atlantic rift. Note, gradual subsidence has occurred since
893 Figure 4A. **D** 54.5-54 Ma. Following commencement of the proto north atlantic rift, the
894 Faroe-Shetland Basin has experienced a loss of dynamic support, resulting in more rapid
895 retreat of the coastline to the south with marine conditions established in the centre of the
896 basin.

897

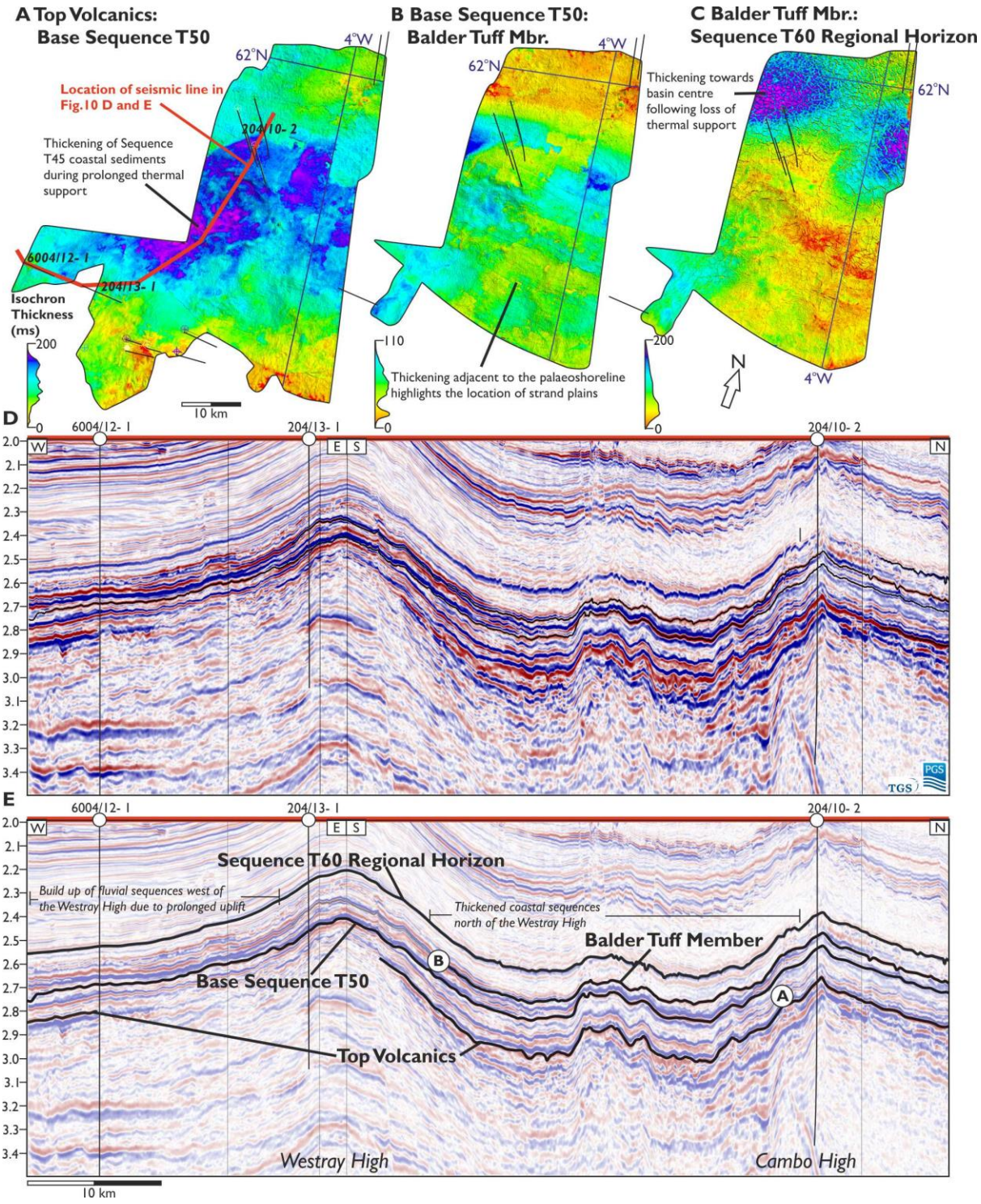

Figure 10. Thickness maps of the Upper Palaeocene to Lower Eocene in the Faroe-Shetland Basin 2011/2012 Geostreamer© survey. Histograms contained within the colour bars show the relative quantity of sediment at each thickness. **A** Isochron thickness from the Top volcanics to the base Sequence T50. **B** Isochron thickness from base Sequence T50 to the Balder Tuff member. **C** Isochron thickness from the Balder Tuff Member to the Sequence

904 T60 softkick. **D** Composite seismic line from the southwest of the study area to the Cambo

905 High. Location of the seismic line shown on Fig. 9A.